Chapter 5

Gravity currents

5.1 Introduction

Gravity currents occur when there are horizontal variations in density in a fluid under the action of a gravitational field. A simple example that can be readily experienced is the gravity current that flows into a warm house through a doorway when it is opened on a cold windless day. The larger density of the cold air produces a higher pressure on the outside of the doorway than on the inside, and this pressure difference drives the cold air in at the bottom and warm air out at the top. If the temperature difference is large enough you will experience a cool draft around your legs if you stand in the doorway.

This example also illustrates a second feature that is needed to produce a gravity current. As shown in figure 5.1 the cool incoming air flows along the hall as a gravity current. The escaping warm air rises up the facade of the building as a turbulent plume. The presence of the floor is need to ensure that the cool air flows horizontally – as would be the case of the warm air if there was a large overhanging balcony.

So, in addition to horizontal density variations, there must also be some feature to stop the fluid from either rising or falling indefinitely and to constrain the flow to be primarily horizontal. In many cases this is a solid boundary, such as the ground. In other situations it may be another feature of the density variations within the fluid, such as a density interface.

Gravity currents occur in gases when there are temperature differences, as in the doorway flow just described. An important atmospheric example is the sea breeze, which is the flow of cool moist air from the sea to the land. On a warm day the sun heats the land more than the sea and, consequently, the air at low altitudes over the land is warmer than that over the sea. The resulting density difference drives the sea breeze. The sea breeze is a significant feature of coastal meteorology in many parts of the world. For example, the wind measured at the Scripps Institution of Oceanography pier in La Jolla, California shows a strong daily signal with a maximum wind directed almost exactly

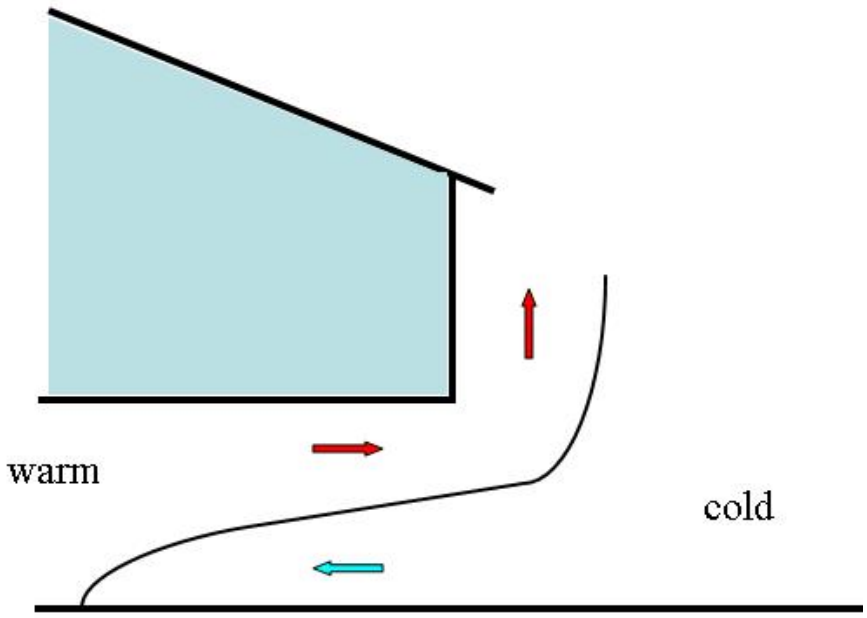

Figure 5.1: A sketch of buoyancy-driven flow through a doorway showing the incoming cold air flowing as a gravity current into the hall. The escaping warm air rises as a turbulent plume since there is no upper boundary to constrain its motion.

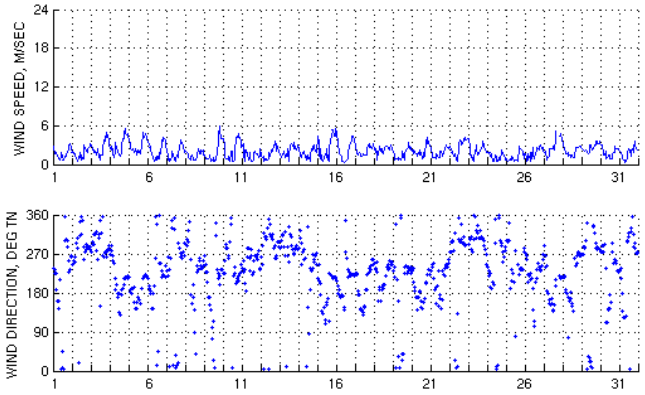

Figure 5.2: Wind speed and direction measured at the Scripps Institution of Oceanography pier in July 2002. Note the clear diurnal cycle with the maximum onshore wind corresponding to the sea breeze.

normal to the coast at 1400 local time during the summer. Figure 5.2 shows the daily variation in the wind speed and direction during July 2002, associated with the sea breeze during the day . This flow ventilates the coastal strip in southern California with cool air, reducing the peak summer temperatures by up to 10^o C from the values observed 20 km inland. This flow affects property prices, which are a (decreasing) function of distance from the coast. Figure 5.3 shows the sea fog being carried in with the sea breeze over Riverside, California in March 1972. Riverside is about 100 km from the coast and this picture shows that the sea breeze can reach far inland, even though at this time of the year the land-sea temperature contrast is quite modest. In some arid regions of the world the effect of the sea breeze has been observed over 1000 km from the coast.

Another important class of gravity currents is the flow of dense gases caused by the accidental release of a liquefied gas. There are many examples of the storage of liquefied gas. Chlorine, commonly used for sterilizing swimming pools, is an example of a toxic gas that is stored in a pressurized container. These containers are found in residential areas, and chlorine is transported by road and rail. Flammable gases such as natural gas and propane are also stored in this way, often in large quantities. If a leak occurs or the container fails catastrophically, the released liquid vaporizes and produces cold gas, which is denser than air because of its low temperature. Even for low molecular weight gases such as methane the effects of temperature dominate and the cold gas will, under most circumstances, produce a gravity current. Because of the potential dangers of a toxic or flammable gas spreading over the ground in populated regions, there has been considerable research into the consequences of such accidental spills over the past 20 years and much of our understanding of

Figure 5.3: The sea breeze over Riverside, California on 16 March 1972. The cold, moist sea air carries photochemical smog picked up on its passage from the coast.

gravity currents comes from field, laboratory and theoretical studies focused on this problem.

In the 1970s Shell carried out a number of field trials on the release of LNG and figure 5.4 shows an example of the cloud that results. In this case the cloud is made visible by the condensation of water vapour in the air as a result of the low temperatures in the cloud. The presence of droplets shows that there is entrainment of the ambient air into the cloud as it forms and flows. This dramatic picture shows a number of remarkable features. Perhaps most noticeable is the sharp front or leading edge, with a convoluted structure. On this front there are smaller scale across-front variations known as 'lobes and clefts' and first described by Simpson (1972). The top of the cloud is quite flat and shows little evidence of mixing with the ambient air.

Figure 5.5 shows a laboratory gravity current, produced when a salt solution propagates into fresh water. The salt water is dyed with milk and the remarkable feature of this photograph is how similar it is to the larger scale atmospheric and dense gas currents shown in the previous figures. Although the laboratory current is at a much lower Reynolds number, the sharp front and the lobes and clefts are clearly visible in the laboratory experiment. Given the difference in scales and Reynolds numbers this similarity suggests that the laboratory experiments can provide good models of large scale gravity currents.

Other examples include gravity currents caused by the suspension of particles in a fluid. Generally, on a horizontal surface, air flows are not sufficiently vigorous to lift particles from the ground, so the source of the flow is usually

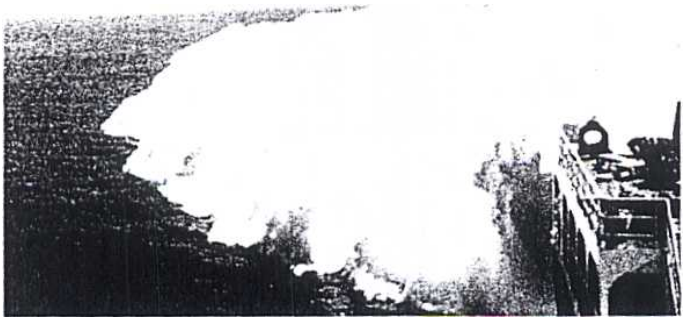

Figure 5.4: A gravity current produced by the discharge of LNG at sea. The current is made visible by the condensation of water vapour within the cold gas cloud.

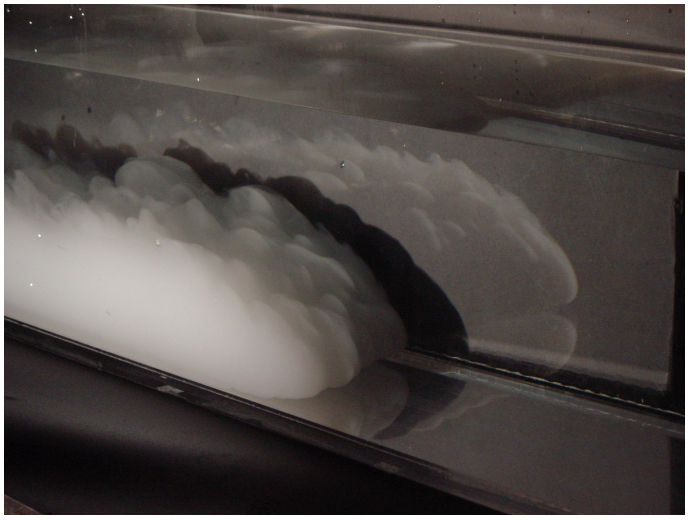

Figure 5.5: A saline laboratory gravity current flowing into fresh water. The current is made visible by milk added to the salt water. The lobes and clefts first reported by Simpson (1972) are clearly visible. The three dimensional structure persists behind the front and affects the structures at the top of the current.

Figure 5.6: A dust storm created by cold air flowing out from under a thunderstorm. This photograph was taken in Leeton, NSW, Australia.

another forcing mechanism such as a cold outbreak from a thunderstorm. Figure 5.6 shows dust suspended in the cold air advancing from underneath a thunderstorm in Leeton, NSW in November 2002 . The front shows the same convoluted structure as that observed in the LNG cloud and also in the laboratory current shown in figure 5.5

The focus of attention for most of the work on gravity currents is the motion of and properties of the front. This is due to the fact that motion near the front is non-hydrostatic and complex in form and so difficult to calculate. This attention also results from the fact that the speed of an oncoming current is essentially the speed of the front. Thus the ability of the vehicle to escape the destruction of the Mount Pinatubo eruption depends on its speed relative to that of the front (see figure 5.7). Similarly a gravity current carries the toxic combustion fumes from a fire in a tunnel, and survival is related to its speed relative to yours.

Although the above examples show that there are many situations where gravity currents occur in natural and industrial flows, there is a more fundamental reason for their study. In a gravitational field, spatial density variations in a fluid produce buoyancy forces. If the density varies in the horizontal direction, flow *always* results. Since, by definition, a fluid can not withstand a finite stress, but is set into motion, a horizontal density variation produces a horizontal pressure gradient which can not be balanced. This is in contrast with vertical variations in density, which produce vertical pressure variations that can be balanced by gravity. Thus a stratified fluid – one where the density varies spatially – can be at rest in a gravitational field only if the density is constant along horizontal planes. Otherwise the fluid will be set in motion.

Figure 5.7: Ash-laden gravity current from the eruption of Mount Pinatubo in 1991. This amazing photograph was taken by Alberto Garcia and is reproduced by permission of the National Geographic. The occupants in the vehicle survived.

5.2 Non-dimensional parameters

The most important non-dimensional parameter for a Boussinesq gravity current is the Froude number F_H , which is defined as the ratio of the current speed U to the long wave speed $\sqrt{g'H}$,

$$F_H = \frac{U}{\sqrt{g'H}}. \tag{5.1}$$

An alternative way of expressing (5.1) is to note that in the absence of viscosity or diffusion, dimensional analysis implies that the velocity of a Boussinesq current is related to its depth H and buoyancy g' by a relationship of the form

$$U = F_H \sqrt{g'H}, \tag{5.2}$$

If these are the only relevant parameters the current will travel at a constant Froude number, suitably defined. In order to determine the value of the Froude number further considerations, either theoretical or experimental, are needed. However, since we expect (5.2) to express the essential balance in the flow it is anticipated that the Froude number F_H is an order one quantity.

The idea that the current travels at a constant Froude number is well supported by experiments, and may be interpreted in a number of ways. These interpretations are not precise, but they are worth discussing briefly.

The first concerns the idea that as the current travels along it derives its energy from the gravitational potential energy stored in the original distribution.

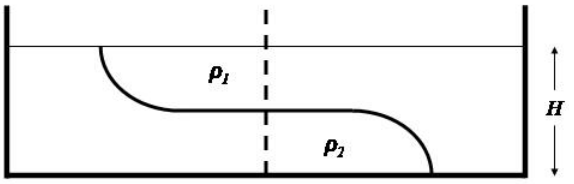

Figure 5.8: A sketch of the idealised of a Boussinesq lock release with symmetrical light and heavy currents. After Yih (1965).

For fluid initially in a lock, the potential energy is reduced as the average depth of dense fluid in the lock decreases as it flows into the current. If this potential energy is converted without loss into the kinetic energy of the current, then we can relate these quantities. The following analysis was first given by Yih (1965).

If we assume that the densities on the two sides of the lock are almost identical (i.e. $\rho_1 \approx \rho_2$ and the current is Boussinesq), then symmetry implies that the current will initially occupy one-half the depth. In a time Δt the fronts will have advanced a distance $U\Delta t$. The potential energy gained by the lighter fluid is $\frac{1}{8}g\rho_1 H^2 U\Delta t$, and that lost by the denser fluid is $\frac{1}{8}g\rho_2 H^2 U\Delta t$. The total kinetic energy gain is $\frac{1}{4}(\rho_1+\rho_2)HU^2 U\Delta t$. Equating these energies gives

$$U = \sqrt{\frac{g(\rho_2-\rho_1)H}{2(\rho_2+\rho_1)}}. \tag{5.3}$$

For the Boussinesq case $\rho_1 \approx \rho_2$, (5.3) implies that $F_H = \frac{1}{2}$. The observed speeds are found to be about 6% less than the theoretical value.

An alternative view of (5.2) concerns the ambient fluid. In a frame of reference moving with the current, and treating the current as a solid obstacle over which the ambient fluid must rise, we can consider the kinetic energy of the flow needed. A balance between the kinetic energy $\frac{1}{2}\rho U^2$ with the required change in potential energy $\frac{1}{2}g\Delta\rho H^2$, gives a value of $F_H = 1$. The idea here is that dissipation is expected to be small in the ambient (as opposed to the current) and so energy conservation has validity.

A different perspective comes from a consideration of the front of a gravity current acting as a hydraulic control. If the current appears is controlled by the flow near the front, it seems reasonable to expect that it is characterised, by analogy with single layer flows, by a critical Froude number. For a two-layer flow the critical condition is

$$F_1{}^2 + F_2{}^2 = 1, \tag{5.4}$$

where the Froude numbers F_i are each based on the respective layer depth H_i.

In the case of a current occupying half the total depth ($H_1 = H_2$) this implies $F_H = \frac{1}{2}$, in agreement with the energy conservation result of Yih (1965). For a current in a deep ambient $H_1 \to \infty, H_2 = H$, (5.4) becomes $F_H = 1$.

The second important parameter is the Reynolds number $Re_H = \frac{UH}{\nu}$, which measures the ratio of inertia to viscous forces. When $Re_H >> 1$, viscous forces are not important and the buoyancy force driving the current is balanced by the inertia of the flow. When $Re_H << 1$, viscous forces provide the main retarding forces to balance the buoyancy forces. Since the transition between these two force balances is gradual, the precise value chosen for the scale H is not too important.

Heat or mass transfer from the current is determined by the Peclet number $Pe_H = \frac{UH}{\kappa}$, where κ is the molecular diffusivity of heat or mass. At high values of $Pe_H >> 1$, molecular transport is not important and instead the density of the current changes, if at all, by mixing with the ambient fluid.

Finally, for non-Boussinesq currents the density ratio $\gamma = \frac{\rho_1}{\rho_2}$ is a further dimensionless parameter that must be considered.

5.3 Scaling analysis

Although gravity-driven fronts occur naturally in fluids with horizontal density gradients, most of our understanding of gravity currents has come from consideration of releases of fluid of one density into a fluid of a second density. Study of these releases is motivated, in part, by the fact that in industrial situations such releases are the possible consequence of the failure of a vessel containing, say, a pressurized gas. It is also easy to produce these flows in the laboratory where gravity currents were first studied.

The main discriminator between these types of releases, is the rate at which the fluid is introduced into the surrounding fluid. In the simplest case, and the one which has received most study, a fixed volume of, say dense, fluid is released from rest into a stationary ambient fluid. This release is known as a *constant volume release*. This kind of release models, for example, the catastrophic failure of a tank containing dense gas, so that the gas is released effectively instantaneously into the air. If, on the other hand, the tank simply ruptured, then the gas would be released at some rate with a volume flux that is a function of time. These releases are known as *flux releases*.

5.3.1 Constant volume releases in a channel

Theory

Consider a finite volume V_0 of dense fluid, density ρ_2, released at $t = 0$ from rest on a horizontal boundary in a stationary ambient fluid of density $\rho_1 < \rho_2$. For simplicity, we assume that the $\rho_1 \approx \rho_2$ so that the flow is Boussinesq. In order to reduce the complexity of the flow, we also suppose the fluid is confined in a channel of unit width, so the dense fluid flows along the channel

and the properties of the flow are independent of the across-channel coordinate. Because of this independence, in a channel the appropriate parameter describing the size of the release is $A_0 = DL_0$, the volume per unit channel width, where D is the depth and L_0 is the length of the initial region of dense fluid. We consider the channel to have a vertical wall at $x = 0$, with the initial region of dense fluid extending from $x = 0$ to $x = L_0$, so that the dense current travels in the positive x direction only, as shown in figure 5.9. The depth of the ambient fluid is H. In laboratory experiments releases of this kind are called lock releases. The dense fluid is contained in a lock by a vertical gate, called the lock gate, and L_0 and D are called the lock length and lock height, respectively. For convenience we will use this nomenclature here.

Flow is generated by the buoyancy force and, for this Boussinesq case, the associated acceleration is given by the reduced gravity $g' = g\frac{\rho_2-\rho_1}{\rho_2}$. As the current propagates it may mix with the ambient fluid and change its density, and we denote the initial negative buoyancy of the dense fluid by ${g'}_0$.

We first consider the case where the initial region of dense fluid is shallow so that $D << L_0$. We also restrict attention to the case where the ambient fluid is very deep, so that $D << L_0 << H$. In the initial phases we suppose that the flow accelerates to a speed large enough that viscous forces are unimportant, and the volume per unit width, A_0, is large enough to be effectively infinite. In that case the only other parameter, apart from ${g'}_0$, determining the flow is the initial depth D of the dense fluid. Dimensional analysis shows that the velocity U of the advancing current at time t is given by

$$U = F({g'}_0 D)^{1/2} f(t/T_a), \tag{5.5}$$

where F is a dimensionless constant and

$$T_a = \sqrt{\frac{D}{g'_0}}, \tag{5.6}$$

is the time scale associated with the acceleration from rest. This time T_a is the free-fall time from a height d with buoyancy ${g'}_0$, and the function $f(t/T_a)$ describes the acceleration from rest. Clearly $f = 0$ when $t/T_a = 0$, and observations (see figure 5.13) show that f tends to a constant, taken as 1 with loss of generality, as $t/T_a \to \infty$. After this acceleration the current travels with a constant speed, characterized by the constant F_D and

$$U = F_D({g'}_0 D)^{\frac{1}{2}}. \tag{5.7}$$

The length $L(t)$ of the current, which is the quantity most easily measured in experiments, is given by

$$L(t) = L_0 + F_D({g'}_0 D)^{\frac{1}{2}} t. \tag{5.8}$$

Since $\sqrt{{g'}_0 D}$ is the speed of infinitesimal long waves on the interface between the two fluids (for $H \to \infty$) and U is the flow speed, F_D, which represents their ratio, may be regarded as a Froude number. As discussed in § 5.2,

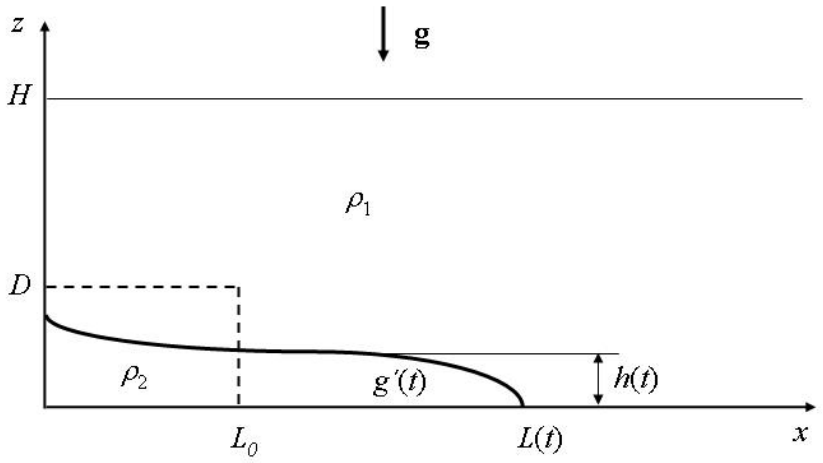

Figure 5.9: A sketch of the release of a finite volume of dense fluid into a less dense stationary environment of depth H. The dense fluid is initially held behind a lock gate at $x = L_0$, and the initial depth is D. The resulting flow is considered to be confined to channel of unit width perpendicular to the plane of the figure.

the front of a gravity current may be thought of as a control in the usual hydraulic sense, and so the notion of it travelling at a constant (critical) Froude number is a reasonable interpretation. The relation (5.5) may also be interpreted as a balance between the buoyancy force driving the current and the inertia of the surrounding ambient fluid, or between the potential energy of the dense fluid and the kinetic energy of the resulting flow. For example, from the horizontal momentum equation (3.17), the balance of the inertia and buoyancy forces may be expressed as $|\mathbf{u} \cdot \nabla \mathbf{u}| \sim g'$. Taking U and D as typical velocity and depth scales, respectively, this implies $U^2 \sim g'D$, consistent with (5.7). The balance between the kinetic and potential energy has been discussed in § 5.2.

At later times, the fact that the volume V_0 of the dense fluid is finite will influence the motion. This introduces a second time scale

$$T_V = \frac{L_0}{\sqrt{g'_0 D}}, \tag{5.9}$$

which is the time it takes a gravity wave with speed $\sqrt{g'_0 D}$ to travel the length L_0 of the lock. After this time the effect of the rear wall of the channel is transmitted by the wave and the finite volume of the lock now becomes a parameter. Then (5.5) becomes

$$U = F_D (g'_0 D)^{1/2} f(t/T_a, t/T_V). \tag{5.10}$$

The variable t/T_V is the dimensionless time associated with the finite volume of the initial release. When t/T_V is small, the current propagates as though the initial volume is infinite, and has a constant speed given by (5.5) in the limit $t/T_a \rightarrow \infty$. This limit requires that $D << L_0$. When t/T_V becomes large, the effects of the finite initial volume become important and the current speed depends only on the negative buoyancy per unit width $B_0 = g'_0 A_0$ and the time t (assuming that viscous effects remain unimportant). Even though the current may mix with its surroundings and reduce its density but increase its volume, conservation of mass implies that B_0 remains constant, provided no fluid is detrained from the current. The dimensions of B_0 are $[B_0]$ = L^3 T^{-2}, and dimensional analysis implies that the length of the current is given by

$$L = cB_0^{\frac{1}{3}} t^{\frac{2}{3}}, \tag{5.11}$$

where c is a dimensionless constant (for high Reynolds numbers). The speed U during this phase decreases as

$$U = \frac{2}{3} cB_0^{\frac{1}{3}} t^{-\frac{1}{3}}. \tag{5.12}$$

Thus dimensional analysis predicts that the current formed from a shallow release initially accelerates to a constant speed. We will see in § **??** that this constant speed regime occurs when fluid is supplied from the lock at a constant rate. Once the finite volume of the lock becomes significant, i.e. when sufficient fluid has flowed away from the release, the speed then decreases as $t^{-\frac{1}{3}}$. In this phase the lock has emptied significantly and the flow of dense fluid from the lock is a decreasing function of time.

The time at which the transition between the constant speed phase and the decelerating phase occurs is found by equating (5.7) and (5.12). This transition time t_s is given by

$$t_s = \left(\frac{2c}{3F}\right)^3 T_V, \tag{5.13}$$

and is the time it takes for the current to propagate a distance equal to a multiple of the lock length L_0.

This time-dependent motion (5.11) is called the *similarity phase* (Simpson (1997)). This result does not assume conservation of volume of the current. The current can mix with the ambient fluid, thereby increasing its volume and decreasing its density. However, the total buoyancy B_0 is conserved, and the speed of the current depends only on B_0, and not individually on g'_0, D or L_0. Thus, at this stage of the motion, the speed of the current is independent of the geometry of the lock, as the effects of the initial conditions (apart from the total buoyancy) are lost.

We can also derive (5.7) and (5.12) by assuming the front travels with a constant *local* Froude number, but now based on the local depth $h(t)$ and the local buoyancy $g'(t)$ at the front (see figure 5.9) rather than the initial values, so that $F = F_h = \frac{U}{\sqrt{g'h}}$.

We represent the current by a characteristic length $L(t)$ and depth $h(t)$ and suppose that it has a uniform buoyancy $g'(t)$. Conservation of buoyancy is expressed as

$$g'(t)L(t)h(t) = c_B g'_0 A_0 = c_B B_0, \tag{5.14}$$

where c_B is a shape constant, which would be unity if the current retained a rectangular shape. A constant local Froude number F_h implies that

$$U = \frac{dL}{dt} = F_h(g'(t)h(t))^{1/2}. \tag{5.15}$$

Using (5.14) and integrating gives

$$L(t) = [\frac{3}{2}F_h(c_B B_0)^{1/2}t + (L_0)^{3/2}]^{2/3}, \tag{5.16}$$

where L_0 is the initial length of the dense fluid in the channel (figure 5.9).

In dimensionless form (5.16) is

$$\frac{L(t)}{L_0} = [\frac{3}{2}F_h {c_B}^{\frac{1}{2}} t/T_V + 1]^{2/3}. \tag{5.17}$$

When $t << T_V$, equation (5.17) gives

$$\frac{L(t)}{L_0} \simeq 1 + F_h {c_B}^{\frac{1}{2}} t/T_V, \tag{5.18}$$

which reduces to (5.8) if $F = F_h {c_B}^{\frac{1}{2}}$. When $t >> T_V$,

$$\frac{L(t)}{L_0} \simeq \left(\frac{3F_h}{2}\right)^{\frac{2}{3}} {c_B}^{\frac{1}{3}} (t/T_V)^{2/3}, \tag{5.19}$$

which gives the same result as (5.11) if $c = \left(\frac{9}{4}c_B {F_h}^2\right)^{\frac{1}{3}}$. The agreement between this calculation and the dimensional analysis supports the assumption that the front of the current travels at a constant local Froude number and, therefore, that the front acts as a control on the flow. Further, it suggests that the same constant Froude number condition may apply to both the constant velocity and decelerating phases of the flow.

As the current decelerates, the Reynolds number decreases and frictional effects become important. The flow is then affected by the viscosity ν of the fluid, which is assumed here to be the same in the current and the ambient fluid. A further time scale

$$T_\nu = \frac{\nu {L_\nu}^2}{{g'}_\nu {h_\nu}^3}, \tag{5.20}$$

now enters the problem, where the subscript ν implies the values of the depth, volume and buoyancy of the current as it enters the viscous phase. These values will, in general, be different from the values of the initial release. Then the front speed may be written as

$$U = F({g'}_\nu h_\nu)^{1/2} f(t/T_a, t/T_V, t/T_\nu). \tag{5.21}$$

The viscous time scale T_ν is the time associated with the diffusion of vorticity over the depth of the current. If we set $T_\nu = \frac{{h_\nu}^2}{\nu}$ then $L_\nu = T_\nu \sqrt{{g'}_\nu h_\nu}$ is the distance a particle will travel in the current in that time. Hence T_ν represents the time at which all the fluid within the current is affected by viscous stresses exerted at the bottom boundary.

At large times we expect the dependence on t/T_a and t/T_V to be unimportant and so $U = f(B_\nu, \nu, t)$. Since there are now three variables and only two dimensions (length and time) it is no longer possible to obtain the speed using dimensional analysis alone. Instead it is necessary to consider the force balances on the current.

In the viscous phase the horizontal pressure gradient driving the current is balanced by viscous stresses so that

$$\frac{\nu}{h^2}\frac{dL}{dt} = \frac{c_\nu {g'}_\nu h(t)}{L(t)}, \tag{5.22}$$

where c_ν is a dimensionless shape constant. To proceed further it is necessary to assume that volume is conserved. This is likely to be a good assumption in the viscous phase when mixing is unimportant, and volume conservation is written as

$$L(t)h(t) = c_A A_\nu, \tag{5.23}$$

where c_A is a further shape constant. Substituting for $h(t)$ from (5.23) and solving the resulting differential equation gives

$$L(t) = [5\frac{c_\nu {c_A}^3 {g'}_\nu {A_\nu}^3}{\nu} t + {L_\nu}^5]^{1/5}, \tag{5.24}$$

where L_ν is the length of the current at the start of the viscous phase.

In dimensionless form (5.24) is

$$\frac{L(t)}{L_\nu} = [5c_\nu {c_A}^3 t/T_\nu + 1]^{1/5}. \tag{5.25}$$

Thus in the viscous phase the current length will increase proportional to $t^{1/5}$. Conservation of volume implies that the depth decreases as $h \sim t^{-\frac{1}{5}}$.

The above analysis shows that, provided the initial acceleration is large enough, the release of a finite volume of dense fluid in a channel will pass through three phases. In the first phase, when the finite volume of the release is unimportant, the speed of the current is constant. After it spreads sufficiently far and the finite volume of the release becomes significant, but the flow is fast enough for viscous forces to be unimportant, the velocity decreases as $t^{-1/3}$. Finally, when viscous forces balance the buoyancy force the current speed decreases as $t^{-4/5}$.

It is possible, of course, that in a very viscous fluid, that viscous effects may dominate from the start of the flow. In that case the first two phases of the flow will be absent, and the flow will be governed by (5.24) at all times. The condition for this to occur is that the initial Reynolds number $Re = \frac{g'^{1/2}D^{3/2}}{\nu}$ of the flow is small.

The above discussion has been restricted to the case where the depth H of the ambient fluid is large compared to both the depth of the initial release d and the local depth of the current h. Where this is not the case, the effect of the flow in the ambient fluid cannot be ignored and the flow depends on a new dimensionless parameter $\Phi \equiv \frac{D}{H}$, called the fractional lock depth. In terms of the scaling analysis given above, this means that the dimensionless constants that appear in the above equations are now dimensionless functions of Φ. In many of the experimental results to be described in the next section $\Phi \sim 1$, while for most environmental flows $\Phi << 1$. Extrapolating the results of the experiments to the case of a deep ambient fluid remains a major challenge in applications to geophysical and environmental flows.

Comparison with experiments

The scaling results in § 5.3.1 leave non-dimensional constants, such as the Froude number, undetermined. In order to determine these constants it is either necessary to develop further theory, as will be done in later chapters, or to determine them from experiments. Here we discuss briefly experiments which test the scaling relations and give values for the constants. As discussed above these 'constants' are, in reality, functions of the depth ratio Φ. There are few experiments that cover a significant range of Φ and so the values obtained have restricted validity. Nevertheless, it is assumed (hoped) that the dependence on the depth ratio is weak, so that the values obtained for relatively small Φ will apply to deeper ambient fluids than are usually tested in the laboratory.

Keulegan (1958) measured the speed of saline gravity currents produced by lock exchange in a channel. His experiments were all full-depth ($\Phi = 1$) lock releases, with the depth of the dense fluid inside the lock the same as the ambient fluid on the other side, and he used two different lock lengths. He found that the speed of the current was constant and independent of the ratio of the channel width and depth, and found a small increase in the Froude number F_H, based on the channel depth H, with Re, from $F_H = 0.42$ at $Re = 600$ to $F_H = 0.48$ at $Re = 150,000$.

Barr (1967) measured the speed of the fronts in a lock exchange for a variety of configurations, and with Reynolds numbers based on the channel depth spanning 200 - 4000. He carried out experiments with both a free and a rigid upper surface, and used temperature and salinity to provide the density difference. Like Keulegan (1958), Barr (1967) also observed that the front of the current travelled at a constant speed, and his results show that the Froude numbers F_H based on the total depth increase with Reynolds number. This variation was most pronounced between Re from 200 - 1000, and there was

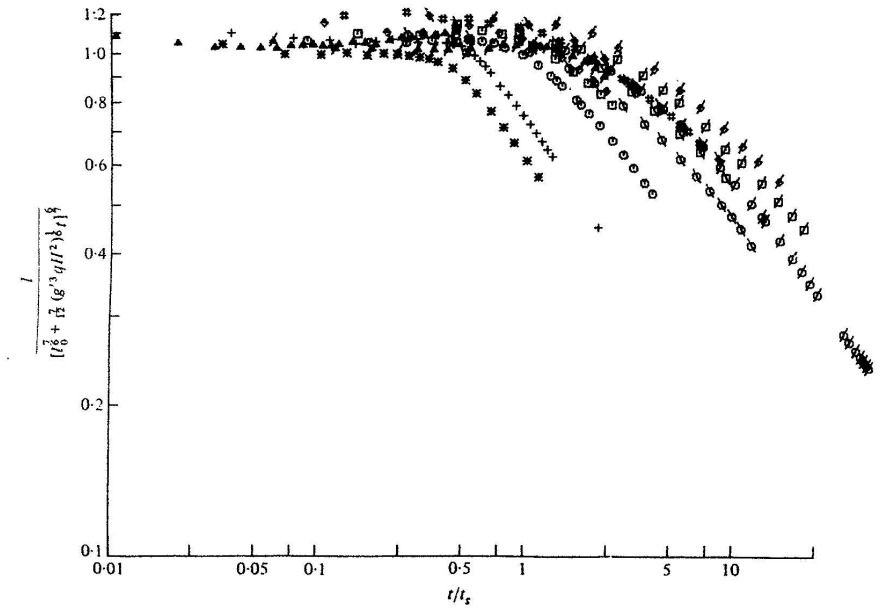

Figure 5.10: The front positions as functions of time after release for a set of experiments with full-depth and partial-depth locks. The length of the current is non-dimensionalised by the right hand side of (5.26) and time by the transition time t_s. In the initial phase the front travels at constant speed after which it decelerates as the similarity phase begins. Taken from Huppert & Simpson (1980).

some slight evidence that little increase in F_H occurs for $Re \geq 1000$. The free surface cases have higher values of F_H. For the rigid upper surface, values of F_H for both currents are comparable, and vary from about 0.42 at Re = 200, to about 0.46 for $Re \geq 1000$.

These results imply that the Froude number $F = \frac{U}{\sqrt{g_0' H}} \approx 0.46 - 0.48$ at high Re when the fractional depth $\Phi = 1$.

Huppert & Simpson (1980) carried out lock exchange experiments that show both the constant velocity and similarity phases of the current. They were concerned with the effects of the fractional depth Φ and present their results in terms of non-dimensional variables that are chosen to fit a particular model in which the local front Froude number decreases with Φ. This makes their results a little difficult to interpret, but from the data shown in figure 5.10 we infer that during the initial phase of the motion

$$L = c\left({L_0}^{\frac{7}{6}} + \frac{7}{12}\left({g_0'}^3 D L_0 H^2 \right)^{\frac{1}{6}} t \right)^{\frac{6}{7}}, \tag{5.26}$$

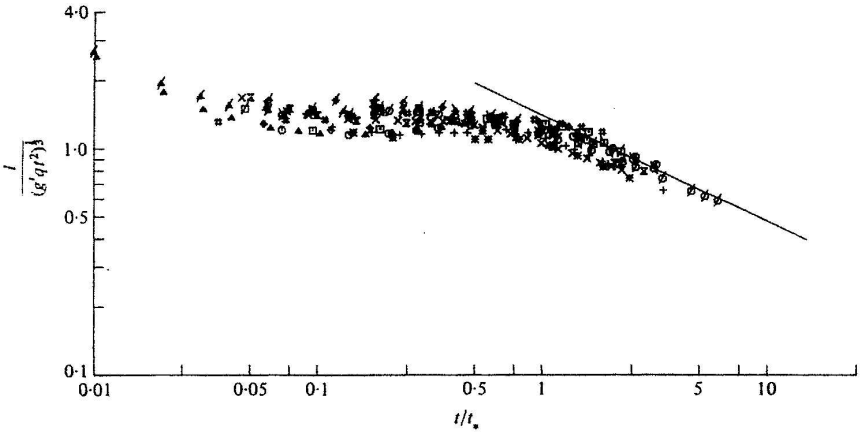

Figure 5.11: The length of Boussinesq currents produced by lock releases in a channel. The length L is scaled by the similarity scaling $B_0{}^{\frac{1}{3}}t^{\frac{2}{3}}$ and the time is non-dimensionalised by the viscous transition time t_1 given by (**??**). Taken from Huppert & Simpson (1980).

where the constant c is about 1.1 (see figure 5.10). Differentiating (5.26) we find that the initial speed is given by

$$U = \frac{dL}{dt} = \tfrac{1}{2}c\Phi^{-\frac{1}{3}}(g_0'D)^{\frac{1}{2}}\left(1 - \frac{(g_0'dD)^{\frac{1}{2}}}{12L_0}\Phi^{-\frac{1}{3}}t\right). \tag{5.27}$$

Hence the current initially travels at a constant speed. Comparison with (5.7) shows that this value of $c = 1.1$ inferred from figure 5.10 gives the Froude number $F = 0.55$ in the limit of a full-depth lock release ($\Phi = 1$). This value is somewhat larger than the value found by Keulegan (1958) and Barr (1967). Huppert & Simpson's data also show that the value of F is a decreasing function of the fractional depth.

Figure 5.11 shows the length of the current non-dimensionalised by $B_0{}^{\frac{1}{3}}t^{\frac{2}{3}}$ as suggested by the similarity scaling (5.11) plotted against non-dimensional time $\frac{t}{t_1}$ defined by (**??**). With this scaling the length is constant in the similarity phase, and from the data we infer the value of the constant c in (5.11) is $c \approx 1.2$. Consequently, the front Froude number F_h (see (5.19)) takes the value

$$F_h = \frac{2}{3}\left(\frac{c^3}{c_B}\right)^{\frac{1}{2}}. \tag{5.28}$$

If the shape factor $c_B = 1$, then this implies that $F_h = 0.88$.

The mechanism whereby the current changes from the constant-velocity to the similarity phase was revealed by Rottman & Simpson (1983). They released dense fluid from a lock of length L_0 and depth D in a less dense ambient fluid

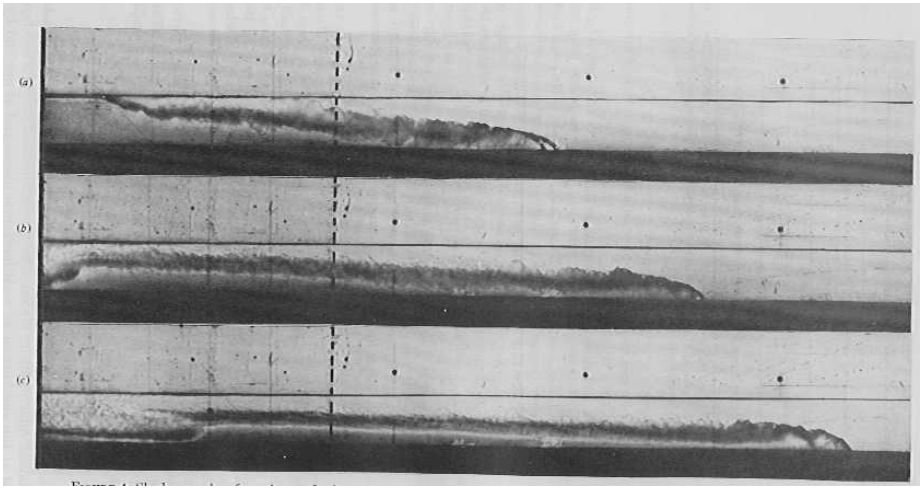

Figure 5.12: Shadowgraphs of a full–depth lock release. The location of the lock gate is shown by the vertical dotted line. In (a) a light surface current is propagating back into the lock. This reflects from the back wall of the lock and forms a bore, seen as the abrupt change in depth at the rear of the current in (b) and (c). Since the bore is behind the front, the front travels at a constant speed, as indicated by its positions in (b) and (c), as the two images are taken at equal time intervals. Taken from Rottman & Simpson (1983).

of depth H. Figure 5.12 shows shadowgraph images of the current for a full depth lock $\Phi = 1$; the position of the lock gate is shown by the dotted vertical line. The lock is shallow, with aspect ratio $\frac{D}{L_0} \simeq 0.16$. The images show the current propagating to the right along the bottom of the tank, and the position of the front (for this and other full-depth releases) is plotted against time in figure 5.13.

Initially the speed of the front is constant; on this log–log plot the slope of distance against time is 1, consistent with (5.7) and confirming that f tends to a constant as $t/T_a \rightarrow \infty$ as discussed in § 5.3.1. Subsequently, the slope decreases so that x increases like $t^{\frac{2}{3}}$, consistent with the results of the scaling analysis (5.19).

For full-depth releases, the transition from the constant–velocity to the self–similar phase occurs at $t \approx 20t_0$ or, equivalently, $L \approx 10L_0$. It is at this point that the influence of the finite volume of the lock becomes important. For that to happen information must travel from the back wall of the lock to the front of the current. This is one instance where the flow in the upper ambient fluid clearly plays an important role. For full–depth releases Rottman & Simpson (1983) show that a finite amplitude bore propagates along the interface, as can

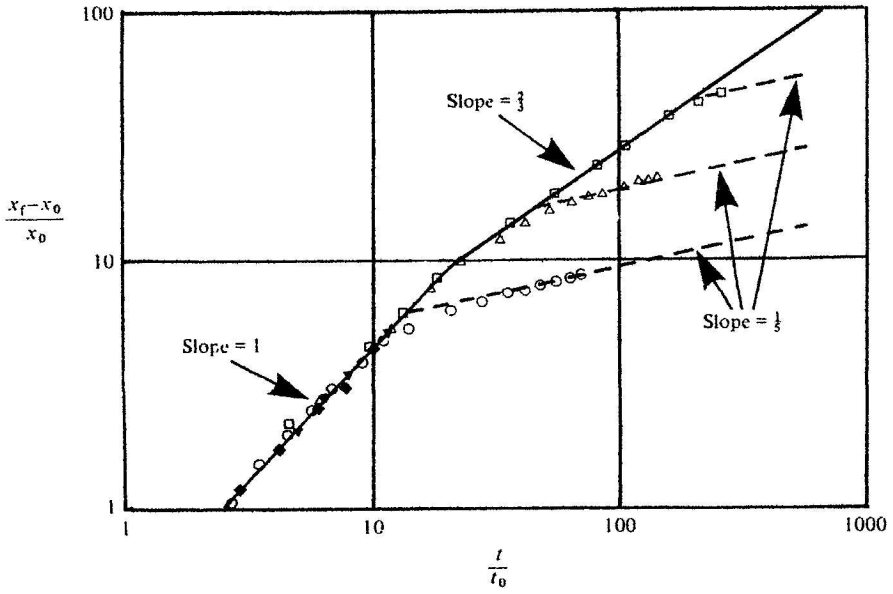

Figure 5.13: A logarithmic plot of dimensionless front positions against dimensionless time for 3 full-depth lock releases. The collapse of the data show that they are well described by (5.5) during the constant velocity phase, when $x \sim t$ and by (5.16) during the similarity phase, when $x \sim t^{\frac{2}{3}}$. The different experiments enter the viscous phase at different times, and then obey (5.24), with $x \sim t^{\frac{1}{5}}$. Taken from Rottman & Simpson (1983).

be seen in the second and third images in figure 5.12. The bore is observed to travel faster than the current head as can be seen in figure 5.14. When the bore catches up with the front, which occurs after the current has travelled about 10 lock lengths, the self–similar phase begins. If the depth of the lock $D < 0.6H$ the disturbance takes the form of a long expansion wave, rather than a bore. In that case experiments show the transition to the similarity phase occurs when the front has travelled a distance x_s of about 3 lock lengths when the $D/H \approx 0$ to about 10 when $D/H = 1$. Hallworth, Huppert, Phillips & Sparks (1996) express this relation empirically as

$$\frac{x_s}{L_0} = 3 + 7.4\frac{D}{H}. \tag{5.29}$$

As the current continues to decelerate, the Reynolds number decreases and viscous effects become increasingly important. Figures 5.11 and 5.13 show that, in the final phase of propagation, the speeds decrease below those observed in the similarity regime. In this final viscous phase, as shown in figure 5.13 by the dashed lines, the front position grows as $t^{\frac{1}{5}}$, as predicted by (5.24).

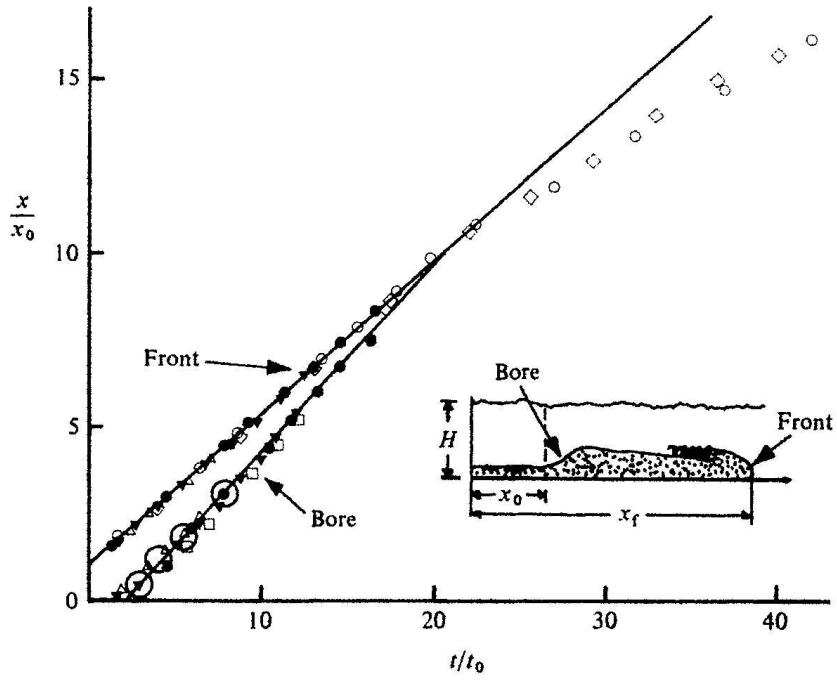

Figure 5.14: The front and bore positions as functions of time after release for a set of experiments with full–depth locks. The straight lines show that the front and bore travel at constant speeds until the bore catches the front, after which the front decelerates. Taken from Rottman & Simpson (1983).

Problem 5.1 *A gravity current is produced by a constant flux of dense fluid in a channel. At the source $x = 0$ the volume flux per unit width is Q_0 and the reduced gravity is g'_0. Use dimensional analysis to show that the front of the current at $x = L(t)$ travels at a constant speed and find the dependence of this speed on Q_0 and g'_0.*

Suppose that the front of the current propagates so that the local Froude number at the front $F = \frac{U}{\sqrt{g'h}}$ is constant. Show that the result is the same as that obtained by dimensional analysis, and calculate the unknown dimensionless constant.

Problem 5.2 *Consider a fluid in which the density is a function of the horizontal coordinate x only, i.e $\rho = \rho(x)$. Draw the isopycnals (surfaces of constant density). Consider the case where the horizontal density gradient is constant so that*

$$\rho = \rho(1 - \alpha x),$$

where $0 < \alpha << 1$ is a constant. Calculate the term giving the baroclinic generation of vorticity $\nabla p \times \nabla \rho$. Find the direction of this vorticity and sketch the anticipated motion of the isopycnals.

Suppose that the flow generated by this density distribution starts from rest and is only in the $x-$direction, i.e. $\boldsymbol{u} = (u, 0, 0)$. Then show that $u = u(z)$ and the inviscid Boussinesq equations of motion are

$$\frac{\partial u}{\partial t} = -\frac{1}{\rho_0}\frac{\partial p}{\partial x},$$

$$g\rho = -\frac{\partial p}{\partial z},$$

$$\frac{\partial \rho}{\partial t} = -u\frac{\partial \rho}{\partial x}.$$

Hence show that

$$\frac{\partial^2 \rho}{\partial x^2} = 0.$$

Solve the initial value problem and show that

$$u = -g\alpha z t,$$

$$\rho = \rho_0(1 - \alpha x) - \tfrac{1}{2} g\rho_0 \alpha^2 z t^2.$$

Finally show that the angle θ of the isopycnals to the vertical satisfies

$$\tan\theta = \tfrac{1}{2} g\alpha t^2,$$

and confirm that this agrees with your earlier sketch.